

RADIAL GATES WITH GATE SILL FOR IRRIGATION STRUCTURES

M. El-Ganainy, M.A. Abourehim and F. El-Fitany

Irrigation and Hydraulics Department, Faculty of Engineering,
Alexandria University, Alexandria, Egypt.

ABSTRACT

Experimental as well as simplified theoretical investigations of the hydraulic characteristics of a radial gate with a gate sill are presented. Variation of the flow coefficient with different geometric and hydraulic parameters is graphically illustrated. Comparison of velocity distributions at three locations downstream the gate shows that energy dissipation produced by relatively low sills is insignificant.

Keywords: Radial gates, Gate sill, Irrigation Structures, Flow coefficient, Velocity distribution.

Notations

- a gate opening;
- B half top length of sill;
- c_c coefficient of contraction;
- F Froude number;
- f head loss coefficient;
- g acceleration due to gravity;
- H_1 upstream head, $H_1 = Y_1 - Z_s$;
- h_1 relative upstream head, $h_1 = H_1/a$;
- H_L energy head loss;
- K flow coefficient;
- q discharge per unit width of the channel;
- R radius of the gate;
- V velocity;
- Y water depth;
- y relative water depth, $y = Y/a$;
- Z_p height of the gate pivot above bottom;
- Z_s height of the sill;
- z_s relative height of the sill, $z_s = Z_s/a$;
- α angle of slope of sill sides; and
- θ lip angle of the gate.

Subscripts

- 1,2,3 upstream, contraction and downstream
- c contracted section.

INTRODUCTION

Radial (tainter or segmental) gates are used extensively in irrigation control structures such as regulators and weirs. They have the advantage of smaller hoist capacity needed, easier operation,

Shukry et al (1992) and Roberson et al (1988), and a better coefficient of discharge, Sehgal (1996). Radial gates were introduced, for the first time, in Egypt in 1985 at the canals of Mansouria in Giza and Talaki in Kalubia.

Previous analytical studies of the hydraulic characteristics of radial gates were very approximate due to several difficulties in hydrodynamic simulation of such gates, Henderson (1970). Experimental studies by Metzler (1948) and Toch (1955) covered a substantial range of values of the independent geometric and hydraulic parameters. Kiselev (1974) presented an experimental formula for the discharge beneath radial gates. Several model studies were carried out to determine more general discharge coefficients for spillway radial gates, U.S. Army Corps of Eng. (1961). Apparently, no study has been made for the hydraulic performance of radial gate with a gate sill in irrigation structures. The construction of such a sill reduces the gate's height, hence it becomes more economic, strengthen the floor section beneath the gate and may be utilized in forming a water cushion downstream (D.S.) of the gate if a second sill is constructed some distance downstream of it.

The current, mainly experimental investigation aims at studying the effect of a radial gate sill on the flow characteristics D.S. of the gate which include the flow coefficient and velocity distributions at several sections. A simplified Theoretical analysis to develop a general formula for the flow coefficient is also presented.

DEFINITION OF THE PROBLEM

The main parameters involved in the current study are illustrated in Figure (1). Geometric parameters are gate radius, R , pivot (trunnion) height, Z_p , gate opening, a , sill height, Z_s , length, $2b$ and slope α . The lip angle, θ , is a function of these parameters:

$$\theta = \cos^{-1} ((Z_p - Z_s - a)/R) \tag{1}$$

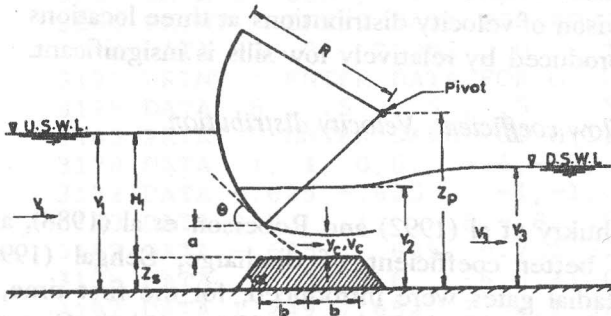


Figure 1. Definition sketch.

Hydraulic parameters include the upstream (U.S.) water depth, Y_1 , the D.S. depth, Y_3 , water depth at the contracted section, Y_2 , the contracted depth, $Y_c = c_c a$, c_c is the coefficient of contraction, and the discharge per unit width of the channel, q .

A dimensional analysis leads to the following functional relationship:

$$f_1 (F_1, \frac{Y_3}{Y_1}, \frac{a}{Y_1}, \frac{R}{Y_1}, \frac{Z_p}{Y_1}, \frac{Z_s}{Y_1}, \frac{b}{Y_1}, \alpha) = 0 \tag{2}$$

in which

$F_1 = q / (Y_1 \sqrt{g Y_1})$, is the Froude number at the U.S. and g is the acceleration due to gravity.

Since values of R , Z_p , b , and α were kept constant throughout the experimental work, the above relationship is simplified to:

$$f_2 (F_1, \frac{Y_3}{Y_1}, \frac{a}{Y_1}, \frac{Z_s}{Y_1}) = 0 \tag{3}$$

If a flow coefficient, K is to be determined from:

$$q = K a \sqrt{2gH_1} \tag{4}$$

in which $H_1 = Y_1 - Z_s$, then a comparison between Eqs. 3 and 4 gives:

$$K = f_3 (\frac{Y_3}{Y_1}, \frac{a}{Y_1}, \frac{Z_s}{Y_1}) = 0 \tag{5}$$

or $K = f_4 (y_1, y_3, z_s) \tag{6}$

in which $y_1 = \frac{Y_1}{a}, y_3 = \frac{Y_3}{a}$ and $z_s = \frac{Z_s}{a}$

EXPERIMENTAL PROCEDURE

Experimental work was performed at the Irrigation and Hydraulics research laboratory, Faculty of Engineering, University of Alexandria. A horizontal rectangular flume, 9.0m long, 0.40m on wide and 0.5 m high was used for that purpose. The flume is provided with a vertical sluice gate at its tail to control the D.S. depth, Figure (2). The radial gate itself is 0.70m radius, satisfying the ratio $R/H_{1, \max} = 1.2$ to 1.5, suggested by Poloncky (1982). The pivot was located at 0.50 m above the bottom in such a way that the gate lip touches the mid-point of the sill when the gate is fully closed. The total sill length, $2b$, is equal to 0.20 m and the U.S. and D.S. slopes of the sill are equal to 45°. A 90° V-notch weir was used to measure the discharge. Velocities at the D.S. were measured by a digital, propeller current meter. Three different heights of the gate sill, $Z_s = 0.0, 0.04$ and 0.08 m, were considered. For each one of these heights different gate openings, $a = 0.02, 0.04, \dots, 0.10$ m, were tested. For a specific opening, four discharges were allowed to flow beneath the gate. Maximum and minimum values of these discharges were restricted by the requirement of submerged flow at the D.S. as well as the height of the flume. For each of these discharges the tail gate is gradually raised till submerged flow conditions D.S. the radial gate is just attained. The corresponding D.S. depth, Y_3^* , is then recorded. As the tail gate is further raised, different combinations of Y_1 and Y_3 , for submerged flow, are obtained and recorded.

For D.S. velocity distribution measurements, only two gate openings, $a = 0.04$ and 0.10 m, were considered, for each height of the gate sill. Two discharge values, $q = 0.01$ and $0.016 \text{ m}^3/\text{s}$, for the first opening, and $q = 0.032$ and $0.036 \text{ m}^3/\text{s}$, for the second one, were used.

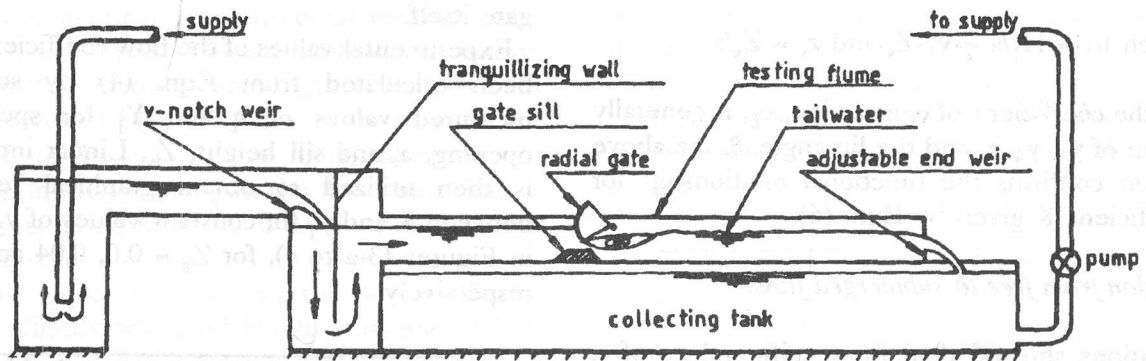


Figure 2. Experimental set-up.

Three vertical sections located at distances $2Y_3$, $4Y_3$ and $6Y_3$ from the D.S. edge of the sill were selected for that purpose. Velocities were measured at depths equal to 0.2, 0.4, 0.6 and 0.8 of the D.S. depth, Y_3 . Additional measurements at 0.007 m below water surface and 0.007 m above the bed were also made. An average of 10 readings of the current meter were taken at each depth.

ANALYSIS AND DISCUSSION

A- Flow Coefficient

A simplified theoretical analysis to determine the flow coefficient for a radial gate with a gate sill is first presented then the experimental results are discussed.

i- Theoretical Investigation:

Referring to Figure (1), the continuity equation between sections 1,2 and 3 yields:

$$q = V_1 Y_1 = V_c Y_c = V_3 Y_3 \quad (7)$$

If pressure distributions at the three sections are assumed to be hydrostatic, the energy equation becomes:

$$\frac{V_1^2}{2g} + Y_1 = \frac{V_c^2}{2g} + (Y_2 - Z_s) + Z_s + H_{L,1,2} = \frac{V_3^2}{2g} + Y_3 + H_{L,2,3} \quad (8)$$

in which $H_{L,1,2}$ is energy losses between sections 1 and 2, and $H_{L,2,3}$ is energy losses between sections 2 and 3.

Application of the momentum equation on the mass of water between sections 2 and 3 results in:

$$\frac{g}{2} (Y_3^2 - Y_2^2) = q (V_c - V_3) \quad (9)$$

In Eqs. (8) and (9) both energy and momentum correction factors have been assumed equal to unity.

Neglecting losses between sections 1 and 2 ($H_{L,1,2}$) and solving Eqs. (7) to (9) for the discharge q , the following relationship is obtained:

$$q = Y_c \sqrt{gaX} \quad (10)$$

in which

$$X = \frac{2}{A} (B - \sqrt{B^2 - 4AC}) \quad (11)$$

with

$$A = [1 - (c_c/y_1)^2]^2, B = 2c_c (1 - c_c/y_3) - y_1 [1 - (c_c/y_1)^2]$$

and

$$C = y_1^2 - y_3^2 \quad (12)$$

Eliminating q between Eqns. (4) and (10) an expression for the flow coefficient, K is obtained:

$$K = c_c \sqrt{\frac{X}{2h_1}} \tag{13}$$

in which $h_1 = H_1/a = y_1 - Z_s$ and $z_s = Z_s/a$

Since the coefficient of contraction, c_c , is generally a function of y_1, y_3, z_s and the lip angle, θ , the above expression confirms the functional relationship for the coefficient K given by Eqn. (6).

Transition from free to submerged flow:

Calculations showed that, for specific values of a, z_s and y_1 the limiting value, y_3^* , at which flow D.S. the gate starts to change from free to submerged conditions corresponds to the special case $B^2=4AC$, hence from Eqn. (11):

$$y_1 = c_c (y_1 - c_c/y_3^*) + y_3^{*2} / [2c_c (1 - c_c/y_3^*)] \tag{14}$$

The corresponding flow coefficient, K^* , is obtained from Eqn. (13):

$$K^* = c_c (y_1^2 - y_3^{*2})^{0.25} / h_1^{0.5} \tag{15}$$

Head loss coefficient:

The head loss, H_L , between sections 1 and 3 may be expressed in terms of the velocity head at the D.S.:

$$H_L = f \left(\frac{v_3^2}{2g} \right) \tag{16}$$

The head loss coefficient, f , can be directly determined from Eqns. (7) and (8):

$$f = (y_3/y_1)^2 - 1 + (2/F_3^2) [(y_1/y_3) - 1] \tag{17}$$

In which $F_3 = q / (Y_3 \sqrt{g Y_3})$, is the D.S. Froude number.

ii- Experimental Results:

It has been noticed that the U.S. water level starts to be affected as soon as the front of the jump reaches the location of the contracted section, section 2 in Figure (1), though gate lip is still free.

Accurate definition of the commencement of submergence should, therefore, refer to the conditions at the contracted section and not at the gate itself.

Experimental values of the flow coefficient, K have been calculated from Eqn. (4) by substituting measured values of q and Y_1 for specific gate opening, a , and sill height, Z_s . Linear interpolation is then utilized to obtain graphical relationship between K and y_1 for constant values of y_3 as shown in Figures (3-a to c), for $Z_s = 0.0, 0.04$ and 0.08 m, respectively.

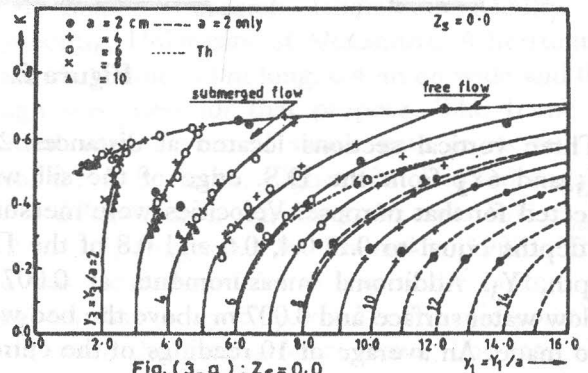


Fig. (3-a) : $Z_s = 0.0$

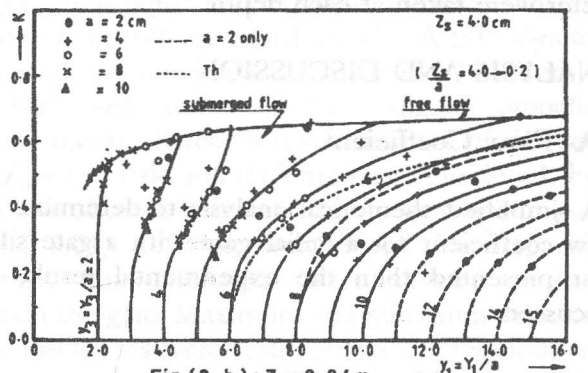


Fig. (3-b) : $Z_s = 0.04$ m

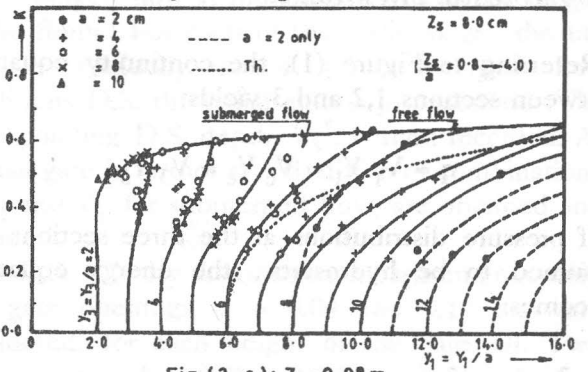


Fig. (3-c) : $Z_s = 0.08$ m

Figure 3. Variation of the flow coefficient (K) with y_1 , and y_3 .

For relatively large gate openings, $a/Y_{1,max} \geq 0.10$, the relative height of the sill, $z_s = Z_s/a$, has a minor effect on the flow coefficient, as indicated by the small deviations of the experimental measurements from the fitted curves. This effect, however, is more significant for relatively small gate openings. The dashed curves in Figures (3-a to c) for $y_3 = 8.0$ and $a = 0.02$ m or $a/Y_{1,max} \approx 0.05$, illustrate the increasing influence of Z_s on the flow coefficient as sill height is raised from 0.0 to 0.04m then to 0.08m, respectively.

For same values of y_1 and y_3 , the flow coefficient increases slightly when sill height is increased from 0.0 to 0.08 m. This does not necessarily mean a mutual increase of the discharge, for same gate opening, since U.S. head, H_1 , used in the simplified discharge equation (4) will decrease simultaneously. Actually, higher sills cause more energy loss U.S. the contracted section while, on the other hand, they reduce the submergence of the issuing jet, as may be concluded from Figure (4). These two factors have opposite effects on the value of the discharge.

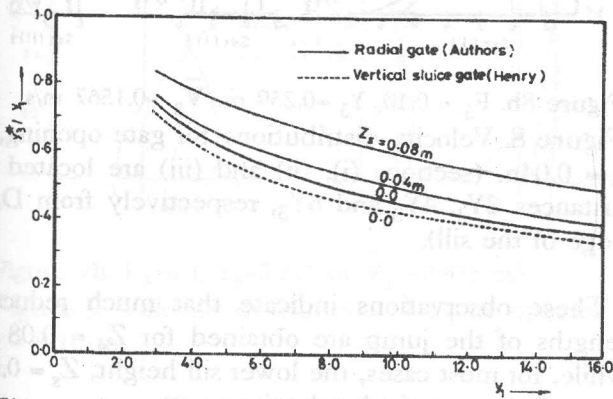


Figure 4. Effect of sill height on free/submerged flow limit.

Theoretical values of the flow coefficient are calculated from Eqn (13) and sample results for $y_3=6.0$ are shown in Figures (3-a to c). Contraction coefficient is approximated by the following expression, Henderson (1970) for free jet without gate sill:

$$c_c = 1 - 0.75 \left(\frac{\theta}{90}\right) + 0.36 \left(\frac{\theta}{90}\right)^2 \quad (18)$$

in which θ is the lip angle in degrees.

Though theoretical ($K-y_1$) relationship has generally similar trends as the experimental one, it consistently produces smaller values of K with an increasing deviation for greater relative U.S. water depths.

Figure (5) shows the variation of the flow coefficient for free afflux, K^* , with the U.S. water depth. Theoretical values determined from Eqn. (15) are also shown.

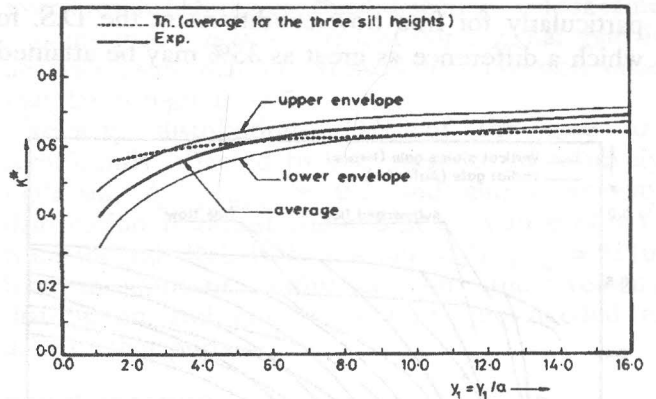


Figure 5. Flow coefficients for free flow conditions.

The head loss coefficient, f , defined by Eqn. (16), is graphically illustrated in Figure (6).

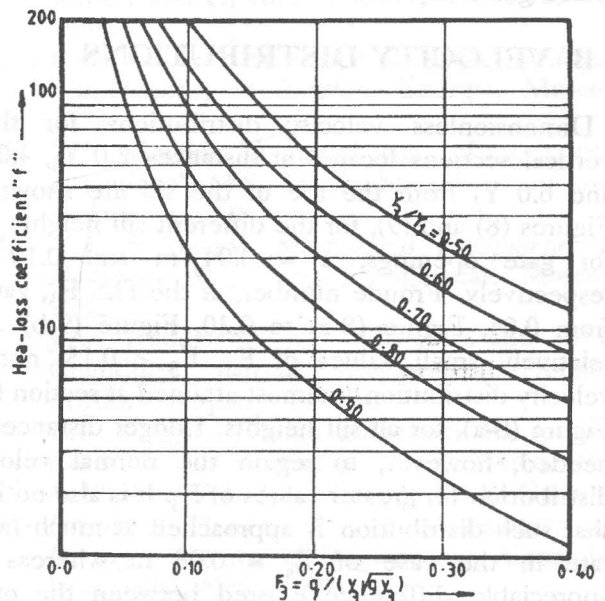


Figure 6. Head-loss coefficient ($f = H_L / (\frac{V_3^2}{2g})$).

Experimentally calculated values of f , for different sill heights as well as experimental observations by Toch (1955), for a radial gate without sill, coincide with this theoretical relationship. This substantiates the assumption of uniform flow conditions at section 1 and 3, Figure (1).

A comparison between current experimental results and those for vertical sluice gate, Henry (1950), with no gate sill, Figure (7), confirms that flow coefficients for radial gates are always greater, particularly for free flow conditions at the D.S. for which a difference as great as 35% may be attained.

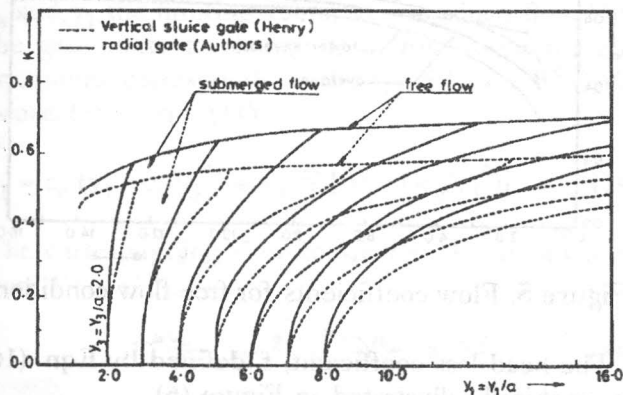


Figure 7. Flow coefficients for radial and vertical sluice gates ($Z_s=0.0$).

B- VELOCITY DISTRIBUTIONS

Dimensionless velocity distributions for three vertical sections located at distances $2.0 Y_3$, $4.0 Y_3$ and $6.0 Y_3$ from the toe of the sill are shown in Figures (8) and (9), for the different sill heights and for gate openings, $a = 0.04$ m and 0.10 m, respectively. Froude number, at the D.S F_3 , varied from 0.04 , Figure (8-a) to 0.30 , Figure (9-b). For relatively small values of F_3 , $F_3 < 0.15$, normal velocity distribution is almost attained at section (iii), Figure (8-a), for all sill heights. Longer distance are needed, however, to regain the normal velocity distribution for greater values of F_3 . It is also noticed that such distribution is approached at much faster rate in the case of $Z_s = 0.08$ m whereas no appreciable difference existed between the other two sills with $Z_s = 0.0$ and 0.04 m. The following table shows approximate lengths of the hydraulic jump formed at the D.S. for different values of Z_s , a and F_3 .

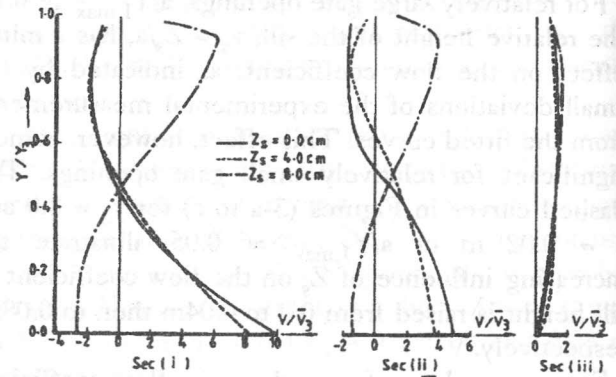


Figure 8a. $F_3 = 0.04$, $Y_3 = 0.345$ m $\bar{V}_3 = 0.0734$ m/s.

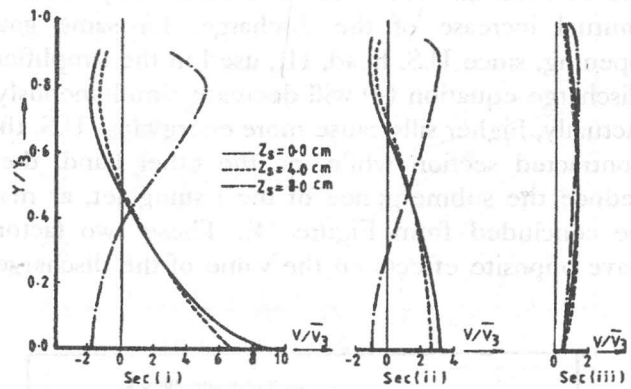


Figure 8b. $F_3 = 0.10$, $Y_3 = 0.259$ m. $\bar{V}_3 = 0.1567$ m/s.
Figure 8. Velocity distributions for gate opening, $a = 0.04$ m (sections (i), (ii) and (iii) are located at distances $2Y_3$, $4Y_3$ and $6Y_3$, respectively from D.S edge of the sill).

These observations indicate that much reduced lengths of the jump are obtained for $Z_s = 0.08$ m while, for most cases, the lower sill height, $Z_s = 0.0$ m produces marginal reduction.

Reverse velocities near the bottom occurred only for the case of $Z_s = 0.08$ m, with a maximum value of $2.7 \bar{V}_3$, Figure (8-a). For $Z_s = 0.0$, maximum bottom velocity reached about $10.0 \bar{V}_3$, Figure (8-a) and slightly lower maximum is attained for a sill height $Z_s = 0.04$ m. Opposite trends are observed for the upper half of the velocity distributions. Excessive forward velocity results from the highest sill used, at 0.70 to 0.92 of the depth whereas reverse velocities exist for the other two sills, at 0.70 to 0.90 of the depth. Since velocity distributions are strongly dependant on the relative location of each

section with respect to the jump itself, these trends are consistent with jump lengths shown in Table (1).

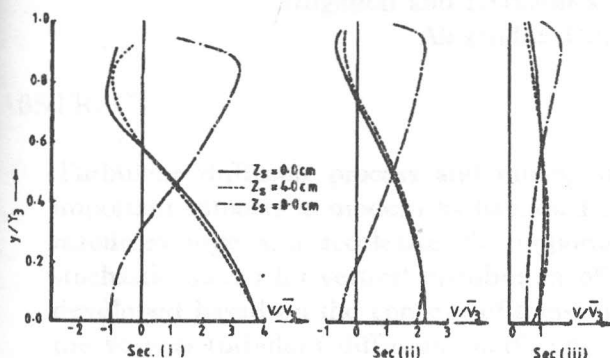


Figure 9a. $F_3=0.15$, $Y_3=0.310$ m, $\bar{V}_3=0.2613$ m/s.

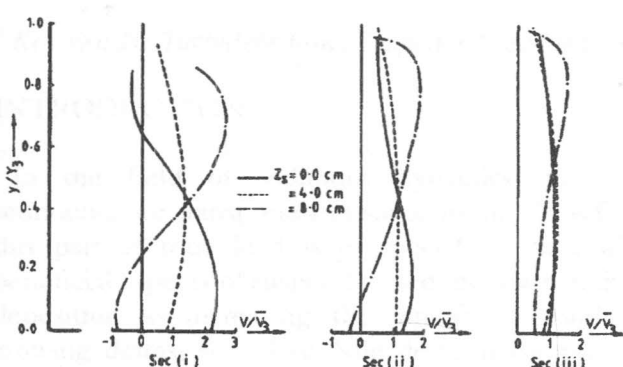


Figure 9b. $F_3=0.3$, $Y_3=0.211$ m, $\bar{V}_3=0.432$ m/s.
Figure 9. Velocity distributions for gate opening, $a = 0.10$ m.

Table 1. Jump lengths.

a (m)	\bar{V} (m/s)	F_3	Z_s (m)		
			0.0	0.04	0.08
0.04	0.073	0.04	1.92	1.49	0.37
	0.157	1.42	1.42	1.36	0.28
0.10	0.261	0.15	1.46	1.40	0.37
	0.432	0.30	0.62	0.20	V. short

CONCLUSIONS

Results of experimental as well as simplified theoretical investigations of the hydraulic characteristics of a radial gate with a gate sill are presented. Variation of flow coefficient, as defined by Eqn. (4), with the sill height, the U.S. and the D.S. water depths for different gate openings and discharges is graphically illustrated in dimensionless form. Higher sills reduce the submergence of the water jet issuing beneath the gate but greater energy losses result U.S. the contracted section. Under same circumstances, flow coefficient for a radial gate is always greater than for a vertical one. The difference may be as high as 35%.

Velocity distributions D.S. of the gate are significantly affected by the presence of relatively high sill, $Z_s/Y_{1,max} \approx 0.2$, and normal velocity distribution is almost attained at a distance of $6 Y_3$ from the sill. Relatively low sill, $Z_s/Y_{1,max} \approx 0.10$, has insignificant influence on the velocity distribution and greater distances are needed to achieve that purpose.

REFERENCES

- [1] F.M. Henderson, *Open Channel flow*, The Macmillan Co., New York, 1970.
- [2] H.R. Henry, "Diffusion of Submerged jets", Discussion by M.L. Albertson, Y.B. Dai, R.A. Jensen and H. Rouse, *Trans. ASCE*, vol. 115, 1950.
- [3] P.G. Kiselev, *Reference Book for Hydraulic Calculations, in Russian*, Energia, Moscow, 1974.
- [4] D.E. Metzler, "A model study of tainter-gate operations", M.S. Thesis, State Univ. of Iowa. Iowa City, 1948.
- [5] G.A. Polonsky, *Mechanical Equipments for Hydraulic Structures*, Energoizdat, Moscow, 1982.
- [6] J.A. Roberson, J.J., Cassidy and M.H. Chaudhry, *Hydraulic Engineering*, Houghton Mifflin Company, Boston, 1988.
- [7] C.K. Sehgal, "Design guidelines for spillway gates", *J. of Hydr. Engrg*, 122 (3), March, 1996.
- [8] A. Shukry, S. El-Khawlika and M. El-Gainy, *Irrigation Design, Part I, Regulators and Barrages*, Faculty of Engineering, Alexandria University, Alex., 1992.
- [9] A. Toch. "Discharge Characteristics of tainter gates", *Trans. of ASCE*, vol. 120, 1955.
- [10] U.S. Army Corps of Engineers, EM 1110-2-1603, 1961.